International Journal of Terrestrial Heat Flow and Applied Geothermics
VOL. 5. NO. 1 (2022); P. 55-61.
ISSN: 2595-4180
DOI: https://doi.org/10.31214/ijthfa.v5i1.87

IJTHFA
http://ijthfa.com/

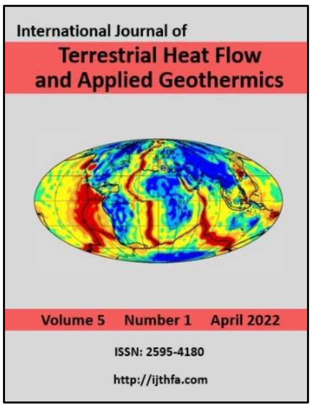

Thermal state of the lithosphere in Eastern Paraguay and in Andean Domain (South American Platform)

Carlos Alexandrino[1], Carlos Mirez[1], André Froede[1], Juliana Batista[1], Carlos Eduardo Nogueira[1]

[1] Instituto de Ciência, Engenharia e Tecnologia, Universidade Federal dos Vales do Jequitinhonha e Mucuri, Teófilo Otoni, Brazil.

Email address

carlos.alexandrino@ufvjm.edu.br (Alexandrino C. H.)
Corresponding author

Keywords

Xenolith Provinces,
Southeast Paraguay,
Andean domain,
Radiogenic heat production,
Heat flow.

Received: February 13, 2022

Accepted: February 16, 2022

Published: April 02, 2022

Abstract

Crustal thermal models that incorporate thermo-barometric data have been developed for estimating depth to 1300 ºC isotherm in two xenoliths provinces: Southeast Paraguay and Andean domain, in South American Platform. Uncertainties in model results has been minimized by imposing reasonable bounds on some of the key model parameters. Considering only the best fit results it is possible to infer average values for geothermal parameters at the surface. This imply heat flow of 86 mWm^{-2}, radiogenic heat production of 1.8 μWm^{-3}. Besides at Moho depth: heat flow of 21 mWm^{-2}, radiogenic heat production of $4.5x10^{-3}$ μWm^{-3}, temperature of from Southeast Paraguay. For the Andean Domain, we have the following values for the geothermal parameters: heat flow, 72 mWm^{-2}, radiogenic heat production, 1.0 μWm^{-3} in surface and heat flow of 33 mWm^{-2}, radiogenic heat production of $2.0x10^{-3}$ μWm^{-3} and temperature of 785ºC in Moho depth. The heat flux estimated for the southeastern Paraguay is higher than that for the Andean domain. This result is in agreement with differences in geological ages between these sites, since the age value for Paraguayan region is approximately 20% lower than the Andean one.

1. Introduction

Mantle derived magmatism and mantle xenoliths of Cretaceous to Early Cenozoic age are the primary sources of information on the thermal and compositional state of the uppermost mantle and lower crust (Kukkonen and Peltonen, 1999; Russell and Kopylova, 1999; Russell et al., 2001; Harder and Russell, 2006; Aulbach et al., 2004; Christophe Michaut, et al., 2007; Howarth et al., 2014; Dymshits et al., 2020), because xenoliths preserve their physical and chemical characteristics while being transported by magmatic processes.

Thus, the method of estimating the thermal field using the thermo-barometric equilibrium condition of xenoliths has become an important means of estimating the thermal regime of the lithosphere for estimating the thermal regime of the lithosphere.

The method was used by Christophe Michaut, et al., 2007; Rudnick, and Nyblade (1999), in a global study with the purpose of investigating the thermal regime in Archaean terrains. Russell et al., (2001) evaluated radiogenic heat production and basal heat flow in the Slave Craton region of Canada on the basis of thermo-barometrical xenoliths data. A similar method also was used by Dymshits et al., (2020) in estimating the thermal state, thickness and composition of the Siberian Craton. These result simply that the information extracted via equilibrium conditions from samples of xenoliths of man-made origin constitutes an efficient way to infer geothermal parameters in the lithosphere, especially in the upper mantle and lower crust.

In this context, the region of eastern Paraguay, within the Andean domain, offers an opportunity to infer geothermal parameters at Moho depth. It is based on the temperature and pressure balance information of upper mantle xenolith samples from data compiled in published work over the past decades (Comin-Chiaramonti et al., 1991, 2001, 2007, 2010; Demarchi et al., 1988; Petrini et al., 1994; Lucassen et al., 2005).

In other words, the objective of this work is to use temperature and pressure information from the mineralogical equilibrium for estimating the thermal state of the lithosphere (lower crust and upper mantle) of Southeast Paraguay. The results maybe as representative of South America Platform and the Andean domain.

2. Geologic Context

Xenoliths and alkaline sodic lavas of Cretaceous to Paleogene period occur in southeastern Paraguay (≈26°S /

≈57°W) and the margins of the Andes (≈26°S / ≈65°W). These locations are indicated in Figure (1) which outlines the study area in simplified form (as referred to in studies of Scheuber and González 1999; Ramos, 2008; Comin-Chiaramonti et al., 1991, 2001; 2007, 2010).

In these regions the tectonic configurations are distinct, while the Andean Domains characterized as a compressible environment. In Southeast Paraguay it is extensible, as indicated by fissures in an intracratonic area. In both locations the host lavas and xenoliths reveal geochemical and isotopic commonalities (Scheuber and González 1999; Ramos, 2008; Comin-Chiaramonti et al., 1991, 2001; 2007, 2010).

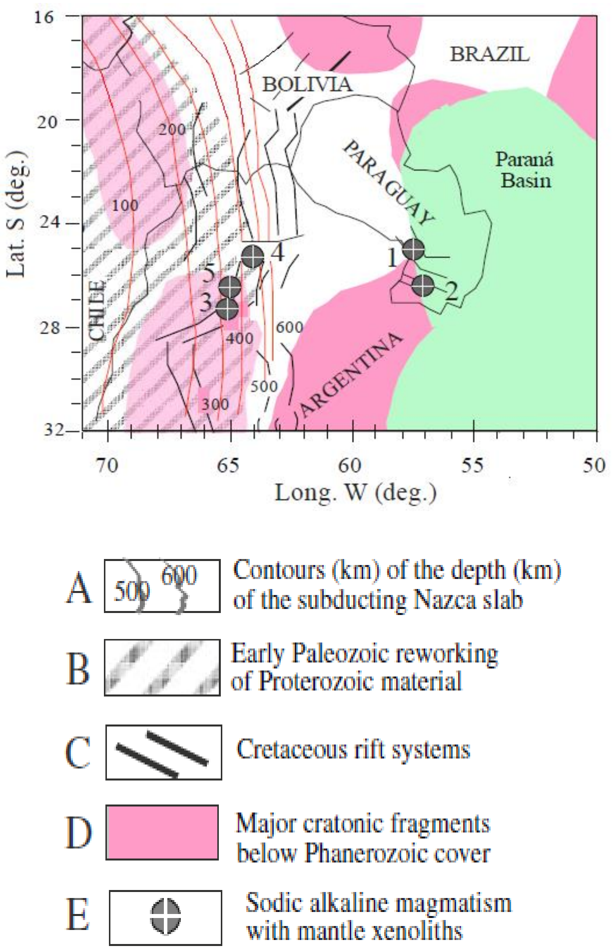

Figure 1 - Map of study region indicating: A, contours of depth in km of subducting Nazca slab based on results of seismic data; B, outlines of Cretaceous rift systems; C, region of extension of intense early Paleozoic reworking of Proterozoic material; D, inferred positions of major cratonic fragments below Phanerozoic cover; E, localities characterized by sodic alkaline magmatism with mantle xenoliths: 1, Asunción (59 Ma) 2, Misiones (118 Ma); 3, Belén (130 Ma); 4, Las Conchas and Cadillal (100 Ma); 5, Finca del Rodeo (96 Ma). (adapted from Comin-Chiaramonti et al. 2007).

There are two main types of xenolith mantle-related suites in the study area, the so-called potassium-poor (LK), and the potassium-rich (HK). The potassium-rich suites occur only in Paraguay. The composition of both suites ranges from lherzolite to dunite, indicating occurrence of melt extraction (Scheuber and González 1999; Taylor et al. 2005; Ramos 2008, Comin-Chiaramonti et al., 2001, 2007; 2009).

3. Materials and Methods

This magmatism locally includes mantle xenoliths (spinel facies) in Paraguay (Misiones and Asunción, Figure (1)) and in Andes (Las Conchas, Figure 1), these mantle xenoliths vary in size from a few centimeters to 45 cm and provide the unique opportunity for a direct sampling of the subcontinental mantle (Lucassen et al., 2005)

Southeastern and central Paraguay, (Figure 1), have the most recent magmatic events in the study area. These events are characterized by alkaline-potassic and alkaline-carbonatite magmatism that occurred from the Lower Cretaceous to the Paleogene (Comin-Chiaramonti et al., 2001, 2007, 2010; Velázquez et al., 2006).

In the Andean domain rock types vary between mafic and ultramafic, with ankaratrites predominating in Finca del Rodeo, and basanites in Las Conchas and Cadillal (Lucassen et al., 2005).

Tables (1) and (2) present the pressure and temperature information, as well as the types of dominant minerals present in xenoliths samples in the Southeast Paraguay and Andean Domain, compiled from various works (Comin-Chiaramonti et al., 2010; Demarchi et al., 1988; Petrini et al., 1994 and Lucassen et al., 2005).

The last column of Table (1) and Table (2) provide sample description. In Table (1) the samples are Alkaline, either potassic or carbonatite. In Table (2) the samples are mafic or ultramafic. Details on the geothermometers and geobarometers used to estimate the pressure and temperature of equilibrium can be consulted in the references from which the information was compiled.

Table 1 - Pressure and Temperature (P-T) data on mantle xenoliths in Southeast Paraguay.

P (kb)	T(°C)	Description
11	841	Alkaline (potassic or carbonatite)
16	881	Alkaline (potassic or carbonatite)
17	963	Alkaline (potassic or carbonatite)
19	971	Alkaline (potassic or carbonatite)
17	975	Alkaline (potassic or carbonatite)
18	978	Alkaline (potassic or carbonatite)
17	979	Alkaline (potassic or carbonatite)
18	983	Alkaline (potassic or carbonatite)
18	988	Alkaline (potassic or carbonatite)
20	990	Alkaline (potassic or carbonatite)
19	995	Alkaline (potassic or carbonatite)
20	1000	Alkaline (potassic or carbonatite)
18	1000	Alkaline (potassic or carbonatite)
19	1003	Alkaline (potassic or carbonatite)
19	1005	Alkaline (potassic or carbonatite)
20	1014	Alkaline (potassic or carbonatite)
20	1028	Alkaline (potassic or carbonatite)
21	1033	Alkaline (potassic or carbonatite)
21	1067	Alkaline (potassic or carbonatite)
20	1104	Alkaline (potassic or carbonatite)
21	1128	Alkaline (potassic or carbonatite)

Table 2 - Pressure and Temperature (P-T) data on mantle xenoliths in the Andean Domain.

P (kb)	T(°C)	Description
17	936	Mafic and Ultramafic
18	995	Mafic and Ultramafic
20	1053	Mafic and Ultramafic
20	1028	Mafic and Ultramafic
20	1020	Mafic and Ultramafic
20	1070	Mafic and Ultramafic
21	1052	Mafic and Ultramafic
21	1087	Mafic and Ultramafic
21	1067	Mafic and Ultramafic
21	1159	Mafic and Ultramafic
21	1119	Mafic and Ultramafic
22	1147	Mafic and Ultramafic
22	1109	Mafic and Ultramafic
22	1115	Mafic and Ultramafic
22	1160	Mafic and Ultramafic
23	1148	Mafic and Ultramafic
23	1126	Mafic and Ultramafic

4. Model Description

According, with Dymshits et al., 2020, Greenfild et al., 2013, Harder and Russell, 2006, Artemieva and Mooney, 2001, Jaupart and Mareschal, 1999; and Russell and Kopylova (1999) among others in the lithosphere the main mode of heat transfer is conduction. Therefore, based on this physical concept, it is possible to develop models to estimate its thermal field based on the following geothermal parameters: heat flux, radiogenic heat production, thermal conductivity and temperature.

The model used in this work, shown in Figure (2), consists of two, and is similar to that proposed by Russell and Kopylova (1999); Harder and Russell, (2006); and Greenfild et al., (2013).

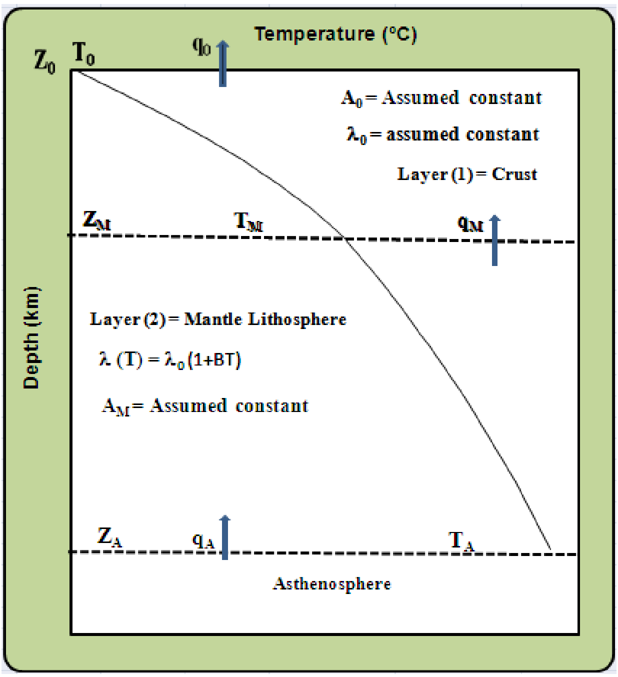

Figure 2 - Schematic representation of model for conductive heat transfer in the crust and mantle lithosphere.

In this figure, layer (1) represents the crust with it stop on the Earth's surface, where Z_0 is considered zero, and the base on the top of mantle at the Z_M position. In this layer the radiogenic heat production A_0 and the thermal conductivity λ_0 are constant. T_0 represents the temperature and q_0 the heat flow, both evaluated at the surface.

The layer (2) represents the lithospheric mantle. The top of this region is indicted as the position of Z_M and its base at the position Z_A. The Moho's depth is Z_M, this way it also represents the crustal thickness. The radiogenic heat production A_M in layer (2) is assumed to be constant, but thermal conductivity $\lambda(T)$ is a function of temperature, while B is the coefficient of variation of thermal conductivity with temperature. T_M and q_M are respectively the temperature and the heat flow at Moho's depth.

The position of Z_A physically represents the thickness of the thermal lithosphere, which is the domain of the lithosphere by definition, where the current main mode of heat transfer is by conduction. In this position the temperature T_A has a value of approximately 1300ºC and q_A represents heat flow from the asthenosphere.

Based on the schematic representation presented in Figure (2) we can formulate the temperature distribution in the lithosphere for the layers (1) and (2) from the one-dimensional equation of heat in permanent regime.

In these conditions equation (1a) can be considered as representative of the thermal field for layer (1). The equation (1b) and (1c) are the contour conditions. In this layer the thermal conductivity and the radiogenic heat production are assumed to be constant.

$$\frac{d^2T_1}{dZ^2} = -\frac{A_0}{\lambda_0} \qquad Z_0 < Z < Z_M \qquad (1a)$$

$$T_1(Z = Z_0) = T_0 \qquad (1b)$$

$$T_1(Z = Z_M) = T_M \qquad (1c)$$

Where T_1 represents the temperature and the other variables are those are those informed previously. The solution to the boundary value problem described by equations (1a) to (1c) is the one described in equation (1d). Equation (1d) describes the temperature distribution for the layer (1).

$$T_1(Z) = -\frac{A_0}{2\lambda_0}Z^2 + \left[\left(\frac{T_M - T_0}{Z_M}\right) + \frac{A_0}{2\lambda_0}Z_M\right]Z + T_0 \qquad (1d)$$

Equation (2a) refers to the formulation for layer (2), where T_2 represents the temperature in this layer. The equations (2b) and (2c) specify the boundary conditions, while equation (2d) indicates the form of variation of thermal conductivity with temperature. The radiogenic heat production in this layer is assumed to be constant, the other variables are as previously informed.

$$\frac{d}{dZ}\left[\lambda(T_2)\frac{dT_2}{dZ}\right] = -A_M \qquad Z_M < Z < Z_A \; (2a)$$

$$T_2(Z = Z_M) = T_M \qquad (2b)$$

$$\lambda(T_2)\frac{dT_2}{dZ} = q_M \qquad (2c)$$

$$\lambda(T_2) = \lambda_0(1 + BT_2) \qquad (2d)$$

Equation (2e), shows the solution for the temperature distribution for layer (2).

$$T_2(Z) = \frac{q_M}{\lambda_0}(Z - Z_M) - \frac{A_M}{2\lambda_0}(Z - Z_M)^2 - \frac{B}{2}[T_2(Z) - T_M]^2 + T_M \quad (2e)$$

The solution of equation (1) was obtained by applying conventional methods for solving differential equations, already the equation (2) was solved by applying Kirchhoff Transform to remove nonlinearity and consequently transform the nonlinear problem into a linear one (For details see Özisik, 1980). This technique was used by Dipple and Kopylova (2000) and Russel et al., (2001) to determine the production and flow of heat in the region of Slave Craton. Canada. Alexandrino and Hamza (2008) used this technique to estimate the thermal field of the Brazilian geological province of San Francisco.

5. Methodology to estimate the geothermal parameters.

In order to use the model proposed in this work is necessary to know some initial conditions. This information is given in Table (3) where T_0 is the average annual surface temperature of the study area. Thermal conductivity λ_0 and density ρ have similar values to those used by Russell and Kopylova (1999), Harder and Russell (2006), and Greenfield et al., (2013). According to Rivadeneyra-Vera et al., (2019) the thickness of the crust in the region varies between 35 to 40 km. Therefore, we assume the average value of 37 km as the characteristic of the crustal thickness of the region.

Table 3 - Physical parameters used in the model.

Parameters	Lithospheric Layers	
	Crust	Mantle
T_0 (ºC)	10	---
Z_M (km)	37	---
λ_0 (W m^{-1} ºC^{-1})	2.5	3.0
ρ (kg m^{-3})	2700	3300

In the following sections we describe the sequential process to estimate the geothermal parameters of interest.

5.1- Geothermal parameters at Moho depth

To estimate the geothermal parameters at the depth of Moho such as temperature T_M, heat flow q_M and radiogenic heat production A_M. For the coefficient of variation of thermal conductivity with temperature B at the depth of Moho we use the pressure and temperature balance data described in tables (1), (2), (3), the physical parameters described in table (4) and equation (4) to form a system of equations.

This system of equations formed from temperature and pressure balance data allowed us to estimate T_M, q_M, A_M and B at Moho depth using appropriate numerical methods. In this work we used the RNLIN routine available in IMSL. The RNLIN routine uses a modified Levenberg-Marquardt method.

5.2 - Radiogenic heat production in the surface A_0.

To estimate heat production at the surface we use equation (1d), thus obtaining equation (3).

$$\frac{dT_1}{dZ}(Z) = -\frac{A_0}{\lambda_0}Z + \left[\left(\frac{T_M - T_0}{Z_M}\right) + \frac{A_0}{2\lambda_0}Z_M\right] \quad (3)$$

We multiply equation (3) by λ_0 and then evaluate it at position $Z=Z_M$. Following this procedure, we arrive at equation (4b) and thus can estimate A_0.

$$\lambda_0 \left.\frac{dT_1}{dZ}\right|_{Z=Z_M} = -\frac{\lambda_0 A_0}{\lambda_0}Z + \lambda_0\left[\left(\frac{T_M - T_0}{Z_M}\right) + \frac{A_0}{2\lambda_0}Z_M\right] \quad (4a)$$

$$A_0 = \frac{2}{Z_M}\left[\lambda_0\left(\frac{T_M - T_0}{Z_M}\right) - q_M\right] \quad (4b)$$

5.3 - Geothermal heat flow at the surface q_0.

To estimate the value of the heat flux at the surface, we first need to multiply eq. (3) by λ_0, and then evaluate it at the position. $Z=Z_0=0$, to obtain the value of the heat flow at the surface.

$$\lambda_0 \left.\frac{dT_1}{dZ}\right|_{Z=Z_0} = -\frac{\lambda_0 A_0}{\lambda_0}Z + \lambda_0\left[\left(\frac{T_M - T_0}{Z_M}\right) + \frac{A_0}{2\lambda_0}Z_M\right] \quad (5a)$$

$$q_0 = \left[\frac{\lambda_0(T_M - T_0)}{Z_M} + \left(\frac{A_0 Z_M}{2}\right)\right] \quad (5b)$$

6. Results and Discussion

Tables (4) and (5) present the results of geothermal parameter estimates. The values of the coefficient of variation of thermal conductivity with temperature and radiogenic heat production in all provinces are compatible with those expected for these parameters (Jaupart and Mareschal, 1999; Kukkonen and Peltonen, 1999; Russell et al., 2001; Artemieva and Mooney, 2001; Dymshits et al., 2020).

Table 4 - Synthesis of model results for geothermal parameters for Southeastern Paraguay.

Parameters	Estimated value			
	Lowe r	Upper	Best	±
T_M (ºC)	764	845	805	41
q_0 (mWm^{-2})	79	90	86	6
q_M (mWm^{-2})	17	28	21	6
A_0 (µWm^{-3})	1.5	2.0	1.8	0.2
A_M (µWm^{-3})	3.5E-03	1.9E-02	6.0E-03	7.8E-03
B (W m^{-1} ºC^{-2})	1.5E-04	1.4E-04	1.8E-04	5.0E-06
Z_A (km)	146	99	120	24

In Southeast Paraguay (see Table - 4) the measured heat flow varies from 79 to 90 mWm^{-2}, and the estimated radiogenic heat value is 1.8 µWm^{-3} at the surface. At Moho depth the temperature and the heat flow have average values of 805ºC and 21 mWm^{-2} respectively and 117 km is the value of the thermal thickness of that region.

For the Andean Domain (Table (5)) the estimated heat flow value at the surface is between 67 to 76 mWm^{-2}. At Moho depth the parameters vary as follows: temperature between 876 to 694 ºC and heat flow from 29 to 38 mWm^{-2}. The average thermal thickness estimated for the province is 86 km, and the estimated surface radiogenic heat production value was 1.8 µWm^{-3}.

Table 5 - Synthesis of model results for geothermal parameters of the Andean Domain.

Parameter	Estimates			
	Lower	Upper	Best	±
T_M (ºC)	694	876	785	91
q_0 (mWm^{-2})	67	76	72	5
q_M (mWm^{-2})	29	38	33	5
A_0 (µWm^{-3})	1.1	0.9	1.0	0.1
A_M (µWm^{-3})	1.0E-03	3.0E-03	2.0E-03	1.0E-03
B (W m^{-1} ºC^{-2})	1.0E-04	2.0E-04	1.1E-04	5.0E-05
Z_A (km)	102	72	86	14

Figures (3) to (4) show the results of the temperature distribution. These figures illustrate the maximum and minimum values of the modelled temperature profiles, as well as the observed data.

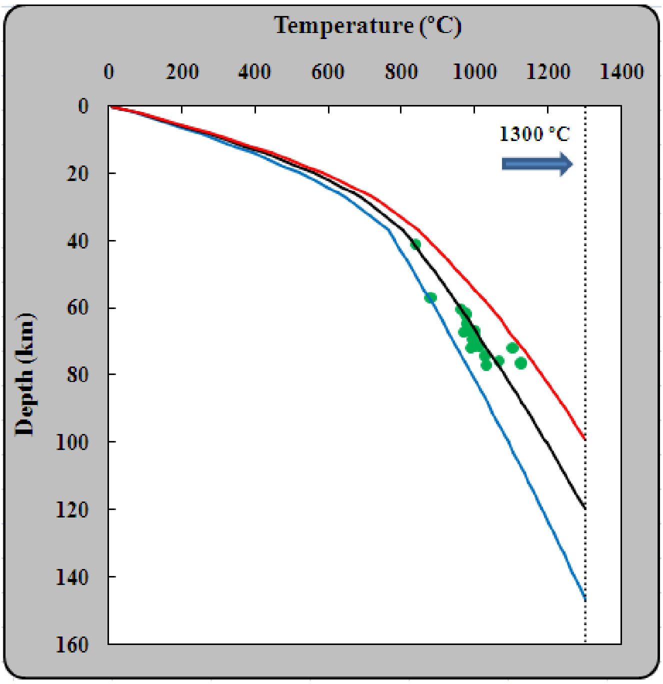

Figure 3 - temperature distribution of the Southeast Paraguay, red line represents the upper limits, blue line the lower limit and black line the best fit. The limits were established with 95% confidence. Gray dotted line represents the isotherm of 1300 ºC and the green dots are the observed data.

The uncertainties in the estimates of the magnitudes listed in Tables (4) and (5) come from a number of sources, including uncertainties of Z_M crustal thickness, pressure, temperature and composition of the xenoliths samples listed in tables (1) and (2) and the value of thermal conductivity λ_0.

To minimize these problems a model of radiogenic heat production and constant thermal conductivity in the crust (layer 1 of Figure 2) and constant heat production in the lithospheric mantle (layer 2 of Figure 2) were chosen in order to reduce the number of variables in the model and consequently obtain more robust results.

Because the value of temperature at the Moho's depth T_M is associated with crustal thickness, and the value of heat flow at the Moho's depth q_M is associated with the value of thermal conductivity, all cases were simulated considering Z_M = 37 km and λ_0 = 3.0 W m^{-1} ºC^{-1} in the lithospheric mantle (layer 2, Figure 3). Therefore, the quantities T_M and q_M (equation 4), are influenced only by the production of A_M radiogenic heat and the coefficient of variation of thermal conductivity B. In relation the production of radiogenic heat in the mantle, the global data indicates that the values of this parameter are in the range of $10^{-6} < A_M < 0.06$ µWm^{-3}. This represents a variation of ± 5.0 ºC in the temperature value T_M and ± 2.0 Wm^{-2} in the value of the heat flow q_M.

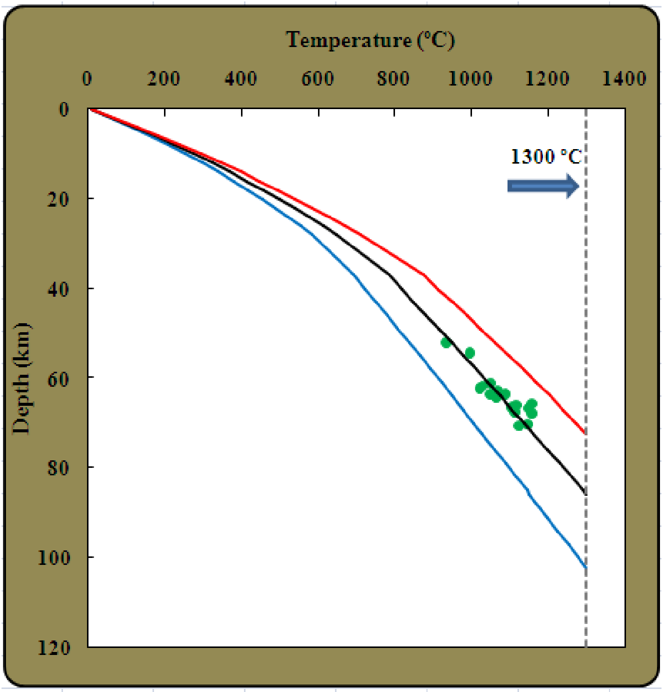

Figure 4 - temperature distribution of the Andean Domain, red line represents the upper limits, blue line the lower limit and black line the best fit. The limits were established with 95% confidence. Gray dotted line represents the isotherm of 1300 ºC and the green dots are the observed data.

The parameter B, according to Kukkonen and Jõeleht, 1995; Seipold, 1998; Jaupart and Mareschal, 1999; Artemieva and Mooney et al., 2001, in the lithospheric mantle their typical values are between $1\text{x}10^{-4} < B < 5\text{x}10^{-4}$ Wm^{-1}ºC^{-2}, which causes a variation of ± 15ºC in the T_M value and in the flow of heat q_M this variation is around ± 4.0 mWm^{-2}.

Figure (5) shows that using the strategy of fixing Z_M and λ_0 refine the values of A_M and B within the range of expected values for these quantities. It was possible to estimate the variables in equation (4) T_M, A_M, q_M, and B in order to obtain the difference between T_{OBS} and T_{MODEL} within the range of uncertainties of the geothermobarometer.

The other constraint used to solve equation (4) was to establish a difference between the observed temperature T_{OBS} and T_{MODEL} below or equal to 20ºC. This value was chosen due to the uncertainty in the thermo-barometry calibration estimated at ± 20 °C and ± 0.3 GPa for the geothermometer proposed by Brey and Kohler, 1990.

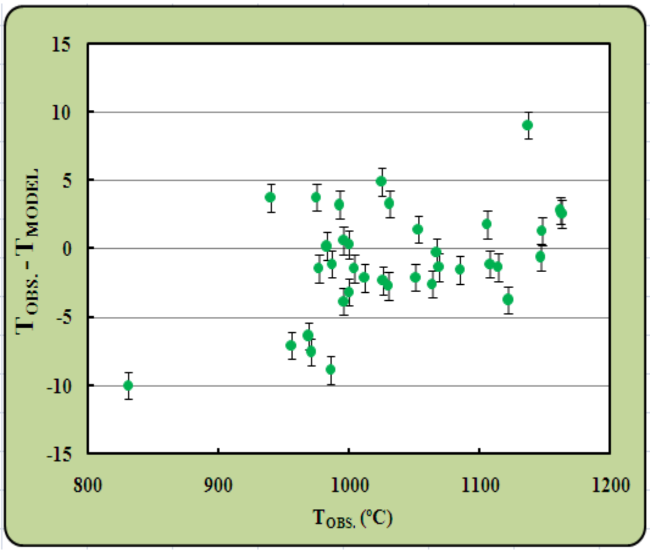

Figure 5 - Residue (difference between observed and modelled temperature) versus observed temperature. The residues are less than 15 ºC.

Imposing these restrictions, we obtain a good quality of adjustment, as can be verified by the analysis of Figure (6) where we can observe a strong correlation between the observed data and that predicted by the model.

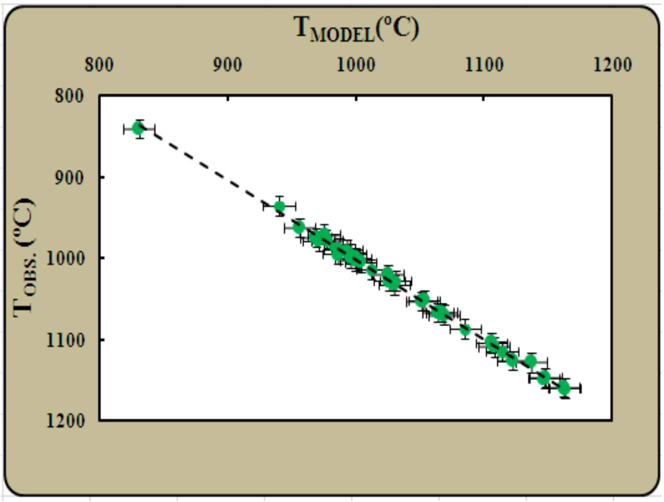

Figure 6 - Relationship between observed and modelled data. The value of R^2 shows strong correlation.

7. Conclusions

The value of heat flow at the surface is similar to that estimated by Vieira and Hamza (2019), Cardoso et al., (2010), Hamza and Muñoz (1996). This agreement was considered as relevant information for validation of the model.

The values of radiogenic heat production and the parameter for variation of thermal conductivity at Moho depth are within the expected range. Hence, we may consider that the model presents coherent results, which indicate the validity of the model when more accurate data are available.

The heat flux estimated for the southeastern Paraguay (86±6 mWm^{-2}) is higher than that for the Andean domain (72± mWm^{-2}).

This result is in agreement with differences in geological ages between these sites, since the age value for Paraguayan region is approximately 20% lower than that for the Andean one.

8. Acknowledgments

Revision of this manuscript benefited from comments by the editorial board of JTHFA.

References

Alexandrino, C.H., Hamza, V.M., 2008, Estimates of heat flow and heat production and a thermal model of the São Francisco Cráton. International Journal of Earth Sciences, Volume 97, Number 2, April 2008, pp. 289-306.

Artemieva, I.M. and Mooney, W.D., Thermal Thickness and Evolution of Precambrian Lithosphere: A Global Study, *J. Geophys. Res.*, 2001, vol. 106, no. B8, pp. 16387–16144.

Aulbach, S.; Griffin, W.L.; O'reilly, S.Y.; McCandless, T.E. Genesis and evolution of the lithospheric mantle beneath the Buffalo Head Terrane, Alberta (Canada). Lithos 2004, 77, 413–451.

Brey, G., Köhler, T. 1990. Geo-thermo-barometry in four-phase lherzolites II. New thermo-barometers, and practical assessment of existing thermo-barometers. Journal of Petrology, 31(6): 1353–1378. doi:10.1093/petrology/31.6.1353.

Christophe Michaut, Claude Jaupart, D. R. Bell. Transient geotherms in Archean continental lithosphere: New constraints on thickness and heat production of the subcontinental lithospheric mantle. Journal of Geophysical Research: Solid Earth, American Geophysical Union, 2007, 10.1029/2006JB004464. insu-01289160.

Comin-Chiaramonti, P., Lucassen, F., Girardi, V. A. V., De Min, A., Gomes, C. B. (2010) Lavas and their mantle xenoliths from intracratonic Eastern Paraguay (South America Platform) and Andean Domain, NW-Argentina: a comparative review. *Mineralogy and Petrology*, 98 (1). 143-165 doi:10.1007/s00710-009-0061-6.

Comin-Chiaramonti P, Marzoli A, Gomes CB et al (2007) Origin of Post-Paleozoic magmatism in Eastern Paraguay. In: RG Foulger and DM Judy (eds) The origin of melting anomalies. Geological Society of America, Special Paper 430, pp. 603–633.

Comin-Chiaramonti P, Princivalle F, Girardi VAA, Gomes CB, Laurora A, Zanetti F (2001) Mantle xenoliths from Ñemby, Eastern Paraguay: O-Sr-Nd isotopes, trace elements and crystal chemistry of hosted clinopyroxenes. Periodico di Mineralogia 70:205–230.

Comin-Chiaramonti P, Civetta L, Petrini R, Piccirillo EM, Bellieni G, Censi P, Bitschene P, Demarchi G, De Min A, Gomes CB, Castillo AMC, Velázquez JC (1991) Cenozoic nephelinitic magmatism in Eastern Paraguay:

petrology, Sr-Nd isotopes and genetic relationships with associated spinel-peridotite xenoliths. Europ J Mineral 3:507–525.

Demarchi, G., Comin-Chiaramonti, P., De Vito, P., Sinigoi, S. and Castillo, C.A.M. (1988). Lherzolite-dunite xenoliths from Eastern Paraguay: petrological constraints to mantle metasomatism. In: The Mesozoic flood volcanism from the Paraná basin (Brazil). (Piccirillo, E.M. and Melfi, A.J., eds.). Iag-Usp, São Paulo, pp 207-227.

Dymshits, A.M.,Sharygin, I.S.,Malkovets, V.G., Yakovlev, I.V., Gibsher, A.A. Alifirova, T.A., Vorobei, S.S., Potapov, S.V., Garanin, V.K., 2020, Thermal State, Thickness, and Composition of the Lithospheric Mantle beneath the Upper Muna Kimberlite Field (Siberian Craton) Constrained by Clinopyroxene Xenocrysts and Comparison with Daldyn and Mirny Fields. *Minerals*, *10*, 549.

Greenfield, A.M.R. Ghent, E.D. Russell, J.K.,2013, Geo-thermo-barometry of spinel peridotites from southern British Columbia: implications for the thermal conditions in the upper mantle. *Canadian Journal of Earth Sciences*; 50 (10): 2013 – 1019 –1032. doi: https://doi.org/10.1139/cjes-2013-0037.

Hamza, V., M. and Muñoz, M., (1996). Heat Flow Map of South America. Geothermics, 25, 599-646. http://dx.doi.org/10.1016/S0375-6505(96)00025-9.

Harder, M., Russell, J.K. 2006, Thermal state of the upper mantle beneath the Northern Cordilleran Volcanic Province (NCVP), British Columbia, Canada. Lithos, 87(1–2): 1–22. doi:10.1016/j.lithos2005.05.002.

Jaupart, C., Mareschal, J. C., 1999, The thermal structure and thickness of continental roots, Lithos, 48, 93– 114.

Kukkonen, I.T., Peltonen, P. 1999, Xenolith-controlled geotherm for the central Fennoscandian Shield: implications for lithosphere-asthenosphere relations. Tectonophysics, 304: 301–315. doi:10.1016/S0040-1951(99)00031-1.

Lucassen, F., Franz, G., Veramonte, J., Romer, R., L., Dulski P., Lang, A., (2005) The late Cretaceous lithospheric mantle beneath the Central Andes: evidence from phase equilibrium and composition of mantle xenoliths. Lithos 82:379–406.

Michaut, C., C. Jaupart, and D. R. Bell (2007), Transient geotherms in Archean continental lithosphere: New constraints on thickness and heat production of the subcontinental lithospheric mantle, J. Geophys. Res., 112, *B04408, doi:*10.1029/2006JB004464.

Pankhurst, R. J., Rapela, C. W. Fanning C.M., Márquez, M. 2006, Gondwanide continental collision and the origin of Patagonia. Earth-Science Reviews, 76, 235–257.

Petrini R, Comin-Chiaramonti P, Vannucci R (1994) Evolution of the lithosphere beneath Eastern Paraguay: geochemical evidence from mantle xenoliths in the Asunción-Ñemby nephelinites. Mineral Petrographica Acta 37:247–259.

Ramos VA (2008) The basement of the central Andes: the Arequipa and related terranes. Ann Ver. Earth Planet Sci. 36: 289–324.

Rivadeneyra-Vera, C., Bianchi, M., Assumpção, M., Cedraz, V., Julià, J., Rodríguez, M., et al. (2019). An updated crustal thickness map of central South America based on receiver function measurements in the region of the Chaco, Pantanal, and Paraná Basins, southwestern Brazil. Journal of Geophysical Research: Solid Earth, 124, 8491- 8505, https://doi.org/10.1029/2018JB016811.

Rudnick, R. L., and A. A. Nyblade (1999), The thickness and heat production of Archean lithosphere: Constraints from xenolith thermoptometry and surface heat flow, in Mantle Petrology: Field Observations and High Pressure Experimentation: A Tribute to Francis R. (Joe) Boyd, edited by C. M. B. Y. Fei, and B.O. Mysen, *pp.* 3–12, The Geochemical Society.

Russell, J.K., Kopylova, M.G., 1999, A steady-state conductive geotherm for the North-central Slave: Inversion of petrological data from the Jericho kimberlite pipe. Journal of Geophysical Research, 104: 7089–7101. doi:10.1029/1999JB900012.

Russell, J.K., Dipple, G.M., Kopylova, M.G., 2001, Heat production and heat flow in the mantle lithosphere to the Slave craton, Canada. Physics of the Earth and Planetary Interiors, 123: 27–44. doi:10.1016/S0031-9201(00)00201-6.

Vieira, F.P. and Hamza, V.M. (2019). Assessment of Geothermal Resources of South America - A New Look, International Journal of Terrestrial Heat Flow and Applied Geothermics, 2, 46-57. DOI: https://doi.org/10.31214/ijthfa.v2i1.32.

Scheuber E, González G (1999) Tectonics of the Jurassic-Early Cretaceous magmatic arc of the north Chilean Coastal Cordillera (22°–26°S): a story of crustal deformation along a convergent plate boundary. Tectonics 18:895–910.

Seipold, U., 1998, Temperature dependence of thermal transport properties of crystalline rocks—a general law. Tectonophysics 291, 161–171.

Velásquez, V. F., Comin-Chiaramonti P., Cundari A, Gomes CB, Riccomini C. (2006). Cretaceous Na-alkaline magmatism from Misiones province (Paraguay): relationships with the Paleogene Na-alkaline analogue from Asunción and geodynamic significance. The Journal of Geology, Vol. 114, No. 5 (2006), pp. 593-614 Published by: The University of Chicago Press http://www.jstor.org/stable/10.1086/506161.